

## **Soret and dufour effects on MHD convective flow of heat and mass transfer over a moving non-isothermal vertical plate with heat generation/absorption**

**M. J. Subhakar<sup>1</sup>, K. Gangadhar<sup>2</sup> and N. Bhaskar Reddy**

<sup>1</sup>*Department of Mathematics, Noble College, Machilipatnam, A.P. 521001, India.*

<sup>2</sup>*Department of Mathematics, ANUOC, Ongole-523001, A.P, India.*

<sup>3</sup>*Department of Mathematics, S. V. University, Tirupati-517502, A.P., India*

---

### **ABSTRACT**

*The present paper is to investigate the effect of linear thermal stratification in stable stationary ambient fluid on steady MHD convective flow of a viscous incompressible electrically conducting fluid along a moving, non-isothermal vertical plate in the presence of mass transfer, Soret and Dufour effects and heat generation or absorption. The governing equations of continuity, momentum and energy are transformed into ordinary differential equations using local similarity transformation. The resulting coupled non-linear ordinary differential equations are solved using Runge-Kutta fourth order method along with shooting technique. The velocity and temperature distributions are discussed numerically and presented through graphs. The numerical values of skin-friction coefficient and Nusselt number at the plate are derived, discussed numerically for various values of physical parameters and presented through Tables. The numerical results are benchmarked with the earlier study by Shrama and Singh [15] and found to be in excellent agreement.*

**Key words:** Heat and Maas transfer, heat generation or absorption, Thermal stratification, MHD, convection, boundary layer flow, non-isothermal plate.

---

### **INTRODUCTION**

Convective heat transfer in thermal stratified ambient fluid occurs in many industrial applications and is an important aspect in the study of heat transfer. If stratification occurs, the fluid temperature is function of distance and convection in such environment exists in lakes, oceans, nuclear reactors where coolant (generally liquid metals) is present in magnetic field etc. Cheesewright [1] examined the natural convection along an isothermal vertical surface in non-isothermal surroundings. Chen and Eichhorn [2] studied natural convection along an isothermal vertical plate in thermally analyzed the effect of magnetic field on natural convection in liquid metal (NaK) used as coolant in nuclear reactor. Venkatachala and Nath [3] obtained the non-similarity solution for natural convection in thermally stratified fluid. Uotani [4] experimentally studied the natural convection in thermally stratification for liquid metal (PbBi). Kulkarni et al. [5] investigated the problem of natural convection from an isothermal flat plate suspended in a linearly stratified fluid medium. Ostrach [6] presented the similarity solution of natural convection along vertical isothermal plate.

The study of magnetohydrodynamic (MHD) flows plays an important role in agriculture, engineering and petroleum industries. The problem of free convection under the influence of a magnetic field has attracted the interest of many researchers in view of its applications in geophysics and astrophysics. Soundalgekar *et al.*[7] analyzed the problem of free convection effects on Stokes problem for a vertical plate under the action of transversely applied magnetic field. Helmy[8] presented an unsteady two-dimensional laminar free convection flow of an incompressible, electrically conducting (Newtonian or polar) fluid through a porous medium bounded by an infinite vertical plane surface of a constant temperature. Zueco[9] analyzed the hydromagnetic convection past a flat plate.

The heat source/sink effects in thermal convection, are significant where there may exist a high temperature differences between the surface (e.g. space craft body) and the ambient fluid. Heat Generation is also important in the context of exothermic or endothermic chemical reaction. Sparrow and Cess [10] provided one of the earliest studies using a similarity approach for stagnation point flow with heat source/sink which vary in time. Pop and Soundalgekar [11] studied unsteady free convection flow past an infinite plate with constant suction and heat source. Hossain *et al.* [12] studied problem of the natural convection flow along a vertical wavy surface with uniform surface temperature in the presence of heat generation/absorption. Chamkha and Khaled [13] obtained similarity solution of natural convection on an inclined plate with internal heat generation/absorption in presence of transverse magnetic field. Molla *et al.* [14] observed the effect of heat generation/absorption on natural convection along a wavy surface. Shrama and Singh [15] have studied the Steady MHD Natural Convection Flow with Variable Electrical Conductivity and Heat Generation along an Isothermal Vertical Plate. Tania *et al* [16] considered the effects of Radiation, Heat Generation and Viscous Dissipation on MHD Free Convection Flow along a Stretching Sheet.

In all these studies Soret / Dufour effects are assumed to be negligible. Such effects are significant when density differences exist in the flow regime. For example when species are introduced at a surface in fluid domain, with different (lower) density than the surrounding fluid, both Soret and Dufour effects can be significant. Also, when heat and mass transfer occur simultaneously in a moving fluid, the relations between the fluxes and the driving potentials are of more intricate nature. It has been found that an energy flux can be generated not only by temperature gradients but by composition gradients as well. The energy flux caused by a composition gradient is called the Dufour or diffusion-thermo effect. On the other hand, mass fluxes can also be created by temperature gradients and this is called the Soret or thermal-diffusion effect. The thermal-diffusion (Soret) effect, for instance, has been utilized for isotope separation, and in mixture between gases with very light molecular weight (H<sub>2</sub>, He) and of medium molecular weight (N<sub>2</sub>, air), the diffusion-thermo (Dufour) effect was found to be of a considerable magnitude such that it can not be ignored (Eckert and Drake [17]). In view of the importance of these above mentioned effects, Dursunkaya and Worek [18] studied diffusion-thermo and thermal-diffusion effects in transient and steady natural convection from a vertical surface, whereas Kafoussias and Williams [19] presented the same effects on mixed free-forced convective and mass transfer boundary layer flow with temperature dependent viscosity. Maleque [20] was discussed by Dufour and Soret Effects on unsteady MHD convective heat and mass transfer flow due to a rotating disk. Sravan *et al.* [21] have analyze the effect of Soret parameter on the onset of double diffusive convection in a Darcy porous medium saturated with couple stress fluid.

The object of the present chapter is to analyze the steady MHD convective flow of a viscous incompressible electrically conducting fluid along a moving, non-isothermal vertical plate by taking mass transfer, Soret and Dufour effects and heat generation or absorption into account. The governing boundary layer equations have been transformed to a two-point boundary value problem in similarity variables and the resultant problem is solved numerically using the forth order Runge-Kutta method along with shooting technique. The effects of various governing parameters on the fluid velocity, temperature, concentration, skin-friction coefficient, Nusselt number and Sherwood number are shown in figures and tables and analyzed in detail.

### MATHEMATICAL ANALYSIS

Consider steady laminar convective flow of a viscous incompressible electrically conducting fluid along a non-conducting, non-isothermal vertical plate moving with constant velocity  $U$ , kept at temperature  $T_w$ , and the ambient fluid far away from plate has temperature  $T_\infty$ . The  $x$ -axis is taken along the plate and  $y$ -axis is normal to the plate. The ambient fluid has temperature  $T_0$  at  $x = 0$ . Magnetic field of uniform intensity  $B_0$  is applied in  $y$  direction. The physical model is given in Figure1. It is assumed that the external field is zero, also electrical field due to polarization of charges and Hall effects are neglected. Incorporating the Boussinesq's approximation within the boundary layer, the governing equations of continuity, momentum, energy and species [Jeffery [22], Bansal [23], Schlichting and Gersten [24]], respectively are given by:

Continuity equation

$$\frac{\partial u}{\partial x} + \frac{\partial v}{\partial y} = 0 \quad (2.1)$$

Momentum equation

$$u \frac{\partial u}{\partial x} + v \frac{\partial u}{\partial y} = \nu \frac{\partial^2 u}{\partial y^2} - \frac{\sigma B_0^2}{\rho} u + g \beta_T (T - T_\infty) + g \beta_c (C - C_\infty) \quad (2.2)$$

Energy equation

$$\rho c_p \left( u \frac{\partial T}{\partial x} + v \frac{\partial T}{\partial y} \right) = k \frac{\partial^2 T}{\partial y^2} + \frac{D_m k_T}{c_s} \frac{\partial^2 C}{\partial y^2} + q(T - T_\infty) \quad (2.3)$$

Species equation

$$u \frac{\partial C}{\partial x} + v \frac{\partial C}{\partial y} = D_m \frac{\partial^2 C}{\partial y^2} + \frac{D_m k_T}{T_m} \frac{\partial^2 T}{\partial y^2} \quad (2.4)$$

The boundary conditions for the velocity, temperature and concentration fields are

$$\begin{aligned} u = U, v = 0, T = T_w = T_0 + bx, C = C_w \quad \text{at } y = 0 \\ u \rightarrow 0, T \rightarrow T_\infty = T_0 + ax, C \rightarrow C_\infty \quad \text{as } y \rightarrow 0 \end{aligned} \quad (2.5)$$

where  $u$ ,  $v$ ,  $T$  and  $C$  are the fluid  $x$ -component of velocity,  $y$ -component of velocity, temperature and concentration respectively,  $\nu$  is the fluid kinematics viscosity,  $\rho$  - the density,  $\sigma$  - the electric conductivity of the fluid,  $\beta_T$  and  $\beta_c$  - the coefficients of thermal and concentration expansions respectively,  $k$  - the thermal conductivity,  $C_\infty$  - the free stream concentration,  $B_0$  - the magnetic induction,  $U_\infty$  - the free stream velocity,  $D_m$  - the mass diffusivity and  $g$  is the gravitational acceleration, and  $C_w$  is the species concentration at the plate surface.

The mass concentration equation (2.1) is satisfied by the Cauchy-Riemann equations

$$u = \frac{\partial \psi}{\partial y}, v = -\frac{\partial \psi}{\partial x} \quad (2.6)$$

where  $\psi(x, y)$  is the stream function.

To transform equations (2.2) - (2.4) into a set of ordinary differential equations, the following similarity transformations and dimensionless variables are introduced.

$$\begin{aligned} \eta = y \sqrt{\frac{U}{\nu x}}, \quad \psi = \sqrt{\nu x U} f(\eta), \quad \theta(\eta) = \frac{T - T_\infty}{T_w - T_\infty}, \quad \phi(\eta) = \frac{C - C_\infty}{C_w - C_\infty}, \quad M = \frac{\sigma B_0^2 x^2}{\mu} (\text{Re})^{-1}, \\ Gr = \frac{g \beta_T (T_w - T_\infty) x}{U^2}, \quad Gc = \frac{g \beta_c (C_w - C_\infty) x}{U^2}, \quad Du = \frac{D_m k_T (C_w - C_\infty)}{\rho c_s c_p (T_w - T_\infty)}, \quad Sr = \frac{D_m k_T (T_w - T_\infty)}{\rho \nu T_m (C_w - C_\infty)}, \\ S = \frac{a}{b} < 1, \quad \nu = \frac{\mu}{\rho}, \quad Pr = \frac{\mu c_p}{k}, \quad Sc = \frac{\nu}{D_m}, \quad Re = \frac{U x}{\nu}, \quad Q = \frac{q x}{U}. \end{aligned} \quad (2.7)$$

where  $\eta$  - similarity variable,  $f$  - dimensionless stream function,  $\theta$  - dimensionless temperature,  $\phi$  - dimensionless concentration,  $M$  - the Magnetic field parameter,  $Gr$  - the thermal Grashof number,  $Gc$  - the solutal Grashof number,  $Du$  - the Dufour number,  $Sr$  - the Soret number,  $S$  - Stratification parameter,  $\nu$  - the kinematic viscosity,  $Pr$  - the Prandtl number,  $Sc$  - the Schmidt number,  $Re$  - the Reynolds number,  $Q$  - heat generation or absorption parameter.

In view of equations (2.6) and (2.7), Equations (2.2) to (2.4) transform into

$$f''' + \frac{1}{2} f f'' + Gr \theta + Gc \phi - M f' = 0 \quad (2.8)$$

$$\theta'' + \frac{1}{2} Pr f \theta' + Pr Du \phi'' + Pr Q \theta = 0 \quad (2.9)$$

$$\phi'' + \frac{1}{2} Sc f \phi' + Sc Sr \theta'' = 0 \quad (2.10)$$

The corresponding boundary conditions are

$$\begin{aligned} f = 0, f' = 1, \theta(0) = 1 - S, \phi = 1 & \quad \text{at} \quad y = 0 \\ f' = 0, \theta = 0, \phi = 0 & \quad \text{as} \quad y = \infty \end{aligned} \quad (2.11)$$

where the prime symbol represents the derivative with respect to  $\eta$  and

Other physical quantities of interest for the problem of this type are the skin friction parameter  $C_f = 2(\text{Re})^{-\frac{1}{2}} f''(0)$ , the plate surface temperature  $\theta(0)$ , Nusselt number  $Nu = -(\text{Re})^{\frac{1}{2}} \theta'(0)$  and the Sherwood number  $Sh = -(\text{Re})^{\frac{1}{2}} \phi'(0)$  (where  $Re = \frac{Ux}{\nu}$  is the Reynolds number). For local similarity case, integration over the entire plate is necessary to obtain the total skin friction, total heat and mass transfer rates.

### SOLUTION OF THE PROBLEM

The set of coupled non-linear governing boundary layer equations (2.8) - (2.10) together with the boundary conditions (2.11) are solved numerically by using Runge-Kutta fourth order technique along with shooting method. First of all, higher order non-linear differential Equations (2.8) - (2.10) are converted into simultaneous linear differential equations of first order and they are further transformed into initial value problem by applying the shooting technique (Jain *et al*[25]). The resultant initial value problem is solved by employing Runge-Kutta fourth order technique. The step size  $\Delta\eta = 0.05$  is used to obtain the numerical solution with five decimal place accuracy as the criterion of convergence. From the process of numerical computation, the skin-friction coefficient, the Nusselt number and the Sherwood number, which are respectively proportional to  $f''(0)$ ,  $-\theta'(0)$  and  $-\phi'(0)$ , are also sorted out and their numerical values are presented in a tabular form.

### RESULTS AND DISCUSSION

The governing equations (2.8) - (2.10) subject to the boundary conditions (2.11) are integrated as described in section 3. Numerical results are reported in the Tables 1-2. The Prandtl number is taken to be  $Pr = 0.71$  which corresponds to air, the value of Schmidt number ( $Sc$ ) were chosen to be  $Sc = 0.24, 0.62, 0.78, 2.62$ , representing diffusing chemical species of most common interest in air like  $H_2$ ,  $H_2O$ ,  $NH_3$  and Propyl Benzene respectively.

The effects of various parameters on velocity profiles in the boundary layer are depicted in Figs. 1-9. It is observed that the velocity starts from a higher value at the plate surface and decrease to the free stream value far away from the plate surface satisfying the far field boundary condition for all parameter values. In Fig. 1 the effect of increasing the magnetic field strength on the momentum boundary layer thickness is illustrated. It is now a well established fact that the magnetic field presents a damping effect on the velocity field by creating drag force that opposes the fluid motion, causing the velocity to decrease. Similar trend of slight decrease in the fluid velocity near the vertical plate is observed with an increase in Stratification parameter ( $S$ ) (see in Fig.2). Fig.3 illustrates the effect of the thermal Grashof number ( $Gr$ ) on the velocity field. The thermal Grashof number signifies the relative effect of the thermal buoyancy force to the viscous hydrodynamic force. The flow is accelerated due to the enhancement in buoyancy force corresponding to an increase in the thermal Grashof number i.e. free convection effects. It is noticed that the thermal Grashof number ( $Gr$ ) influence the velocity field almost in the boundary layer when compared to far away from the plate. It is seen that as the thermal Grashof number ( $Gr$ ) increases, the velocity field increases. The effect of mass (solutal) Grashof number ( $Gc$ ) on the velocity is illustrated in Fig.4. The mass (solutal) Grashof number ( $Gc$ ) defines the ratio of the species buoyancy force to the viscous hydrodynamic force. It is noticed that the velocity increases with increasing values of the solutal Grashof number. Further as the mass Grashof number ( $Gc$ ) increases, the velocity field near the boundary layer increases.

Fig.5 illustrates the effect of the Schmidt number ( $Sc$ ) on the velocity. The Schmidt number ( $Sc$ ) embodies the ratio of the momentum diffusivity to the mass (species) diffusivity. It physically relates the relative thickness of the hydrodynamic boundary layer and mass-transfer (concentration) boundary layer. It is noticed that as Schmidt number ( $Sc$ ) increases the velocity field decreases. Fig.6 illustrates the effect of Prandtl number ( $Pr$ ) on the velocity. It is noticed that as the Prandtl number ( $Pr$ ) increases, the velocity increases. As seen in the earlier cases, far away from the plate, the effect is much significant. Fig. 7 shows the variation of the velocity boundary-layer with the heat generation/absorption parameter ( $Q$ ). It is noticed that the velocity boundary layer thickness increases with an increase in the heat generation/absorption parameter. Fig. 8 shows the variation of the velocity boundary-layer with the Dufour number ( $Du$ ). It is observed that the velocity boundary layer thickness increases with an increase in the

Dufour number. Fig. 9 shows the variation of the velocity boundary-layer with the Soret number ( $Sr$ ). It is found that the velocity boundary layer thickness increases with an increase in the Soret number.

As per the boundary conditions of the flow field under consideration, the fluid temperature attains its maximum value at the plate surface and decreases exponentially to the free stream zero value away from the plate. This is observed in Figs. 10-18. The effect of the magnetic parameter ( $M$ ) on the temperature is illustrated in Fig.10. It is observed that as the magnetic parameter increases, the temperature increases. Fig.11 illustrates the effect of the Stratification parameter ( $S$ ) on the temperature. It is noticed that as Stratification parameter increases, the temperature decreases. From Figs. 12 and 13, it is observed that the thermal boundary layer thickness decreases with an increase in the thermal or Solutal Grashof numbers ( $Gr$  or  $Gc$ ). Fig. 14 illustrates the effect of Schmidt number ( $Sc$ ) on the temperature. It is noticed that as the Schmidt number ( $Sc$ ) increases an increasing trend in the temperature field is noticed. Much of significant contribution of Schmidt number ( $Sc$ ) is noticed as we move far away from the plate.

The effect of Prandtl number ( $Pr$ ) on the temperature field is illustrated Fig.15. As the Prandtl number ( $Pr$ ) increases the thermal boundary layer is found to be increasing. Fig.16 illustrates the effect of the heat generation or absorption parameter ( $Q$ ) on the temperature. It is noticed that as the heat generation or absorption parameter increases, the temperature increases. Fig. 17 shows the variation of the thermal boundary-layer with the Dufour number ( $Du$ ). It is noticed that the thermal boundary layer thickness increases with an increase in the Dufour number. Fig. 18 shows the variation of the thermal boundary-layer with the Soret number ( $Sr$ ). It is observed that the thermal boundary layer thickness decreases with an increase in the Soret number.

Figs. 19-27 depict chemical species concentration against span wise coordinate  $\eta$  for varying values physical parameters in the boundary layer. The species concentration is highest at the plate surface and decrease to zero far away from the plate satisfying the boundary condition. The effect of magnetic parameter ( $M$ ) on the concentration field is illustrated Fig.19. As the magnetic parameter increases the concentration is found to be increasing. However, as we move away from the boundary layer, the effect is not significant. The influence of the Stratification parameter ( $S$ ) on the concentration field is shown in Fig.20. It is noticed that the concentration decreases monotonically with the increase of the Stratification parameter. The effect of buoyancy parameters ( $Gr, Gc$ ) on the concentration field is illustrated Figs. 21 and 22. It is noticed that the concentration boundary layer thickness decreases with an increase in the thermal or Solutal Grashof numbers ( $Gr$  or  $Gc$ ). Fig. 23 illustrates the effect of Schmidt number ( $Sc$ ) on the concentration. It is noticed that as the Schmidt number ( $Sc$ ) increases, there is a decreasing trend in the concentration field. Not much of significant contribution of Schmidt number ( $Sc$ ) is noticed as we move far away from the plate.

The influence of the Prandtl number ( $Pr$ ) on the concentration field is shown in Fig.24. It is noticed that the concentration decreases monotonically with the increase of the Prandtl number. The influence of the heat generation or absorption parameter ( $Q$ ) on the concentration field is shown in Fig.25. It is noticed that the concentration decreases monotonically with the increase of the heat generation or absorption. Fig. 26 shows the variation of the concentration boundary-layer with the Dufour number ( $Du$ ). It is observed that the concentration boundary layer thickness decreases with an increase in the Dufour number. Fig. 27 shows the variation of the concentration boundary-layer with the Soret number ( $Sr$ ). It is found that the concentration boundary layer thickness increases with an increase in the Soret number ( $Sr$ ).

In order to benchmark our numerical results, the present results for the  $\theta'(0)$  in the absence of  $M, Gr, Gc, Sc, Du, Sr, S$ , are compared with those of Shrama and Singh [15] and found them in excellent agreement as demonstrated in Table 1. From Table 2, it is observed that the local skin-friction coefficient, local heat and mass transfer rates at the plate increases with an increase in the buoyancy forces or Dufour number or Soret number or heat generation/absorption parameter. As the Schmidt number increases, both the skin-friction and Nussel number decrease, whereas the Sherwood number increases. It was found that the local skin-friction coefficient and local mass transfer rate at the plate decreases but Nussel number increases with an increase in the Prandtl number. It was observed that the local skin-friction coefficient, local heat and mass transfer rates at the plate decreases with an increase in the Magnetic parameter or Stratification parameter.

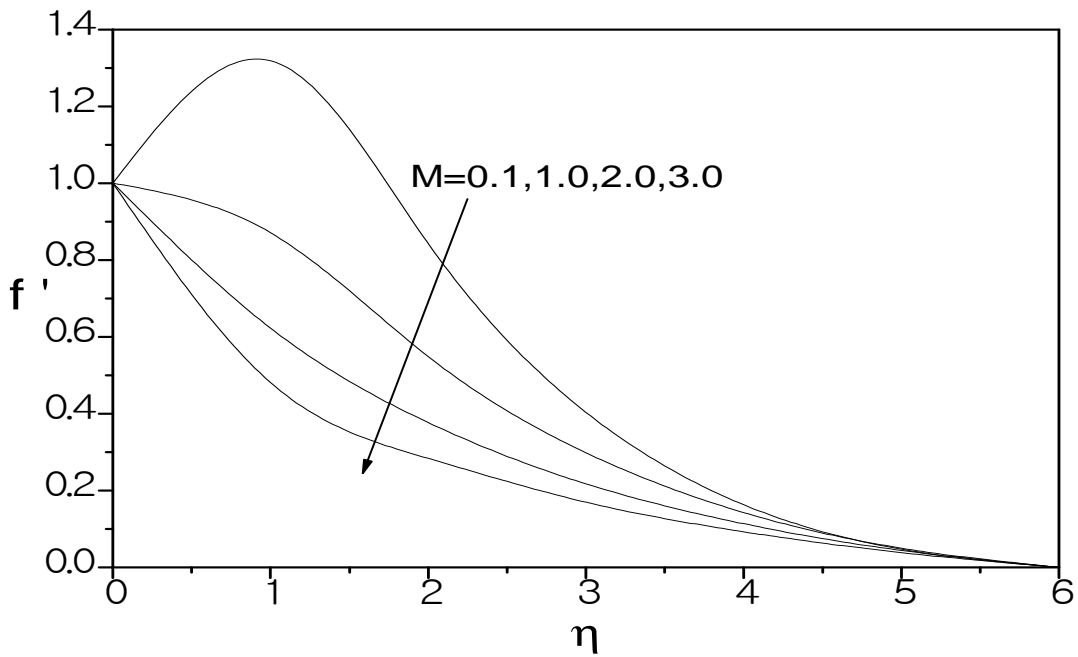


Fig.1: Variation of the velocity  $f'$  with  $M$  for  $Pr=0.71, Sc=0.24, Gr=Gc=0.1, S=0.2, Du= Sr=Q=0.1$ .

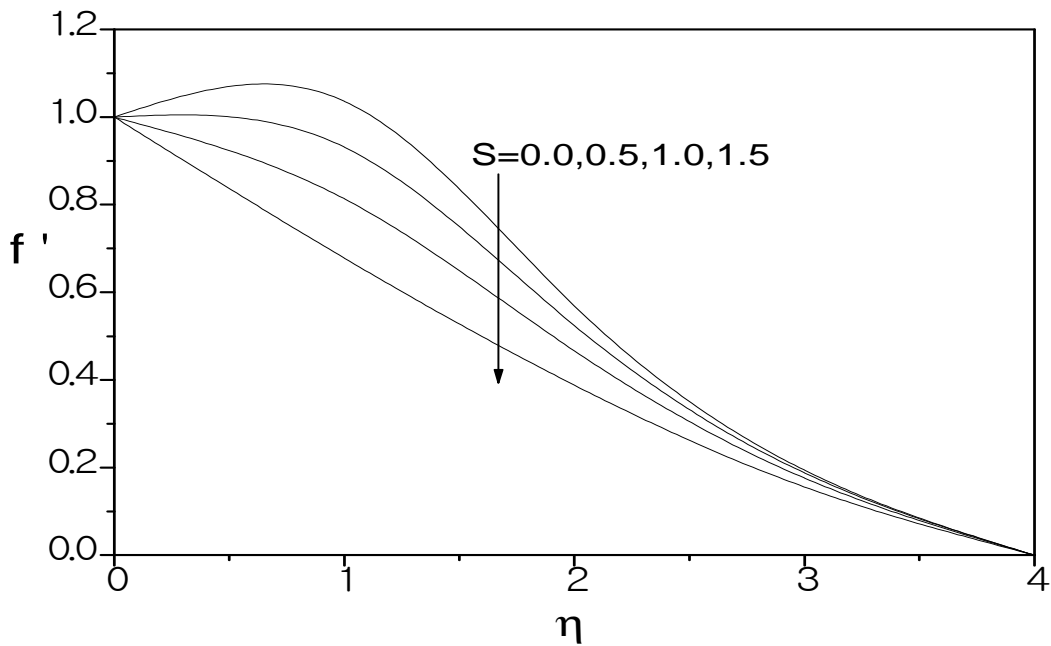


Fig.2: Variation of the velocity  $f'$  with  $S$  for  $Pr=0.71, Sc=0.24, Gr=Gc=0.1, M=0.5, Du= Sr=Q=0.1$ .

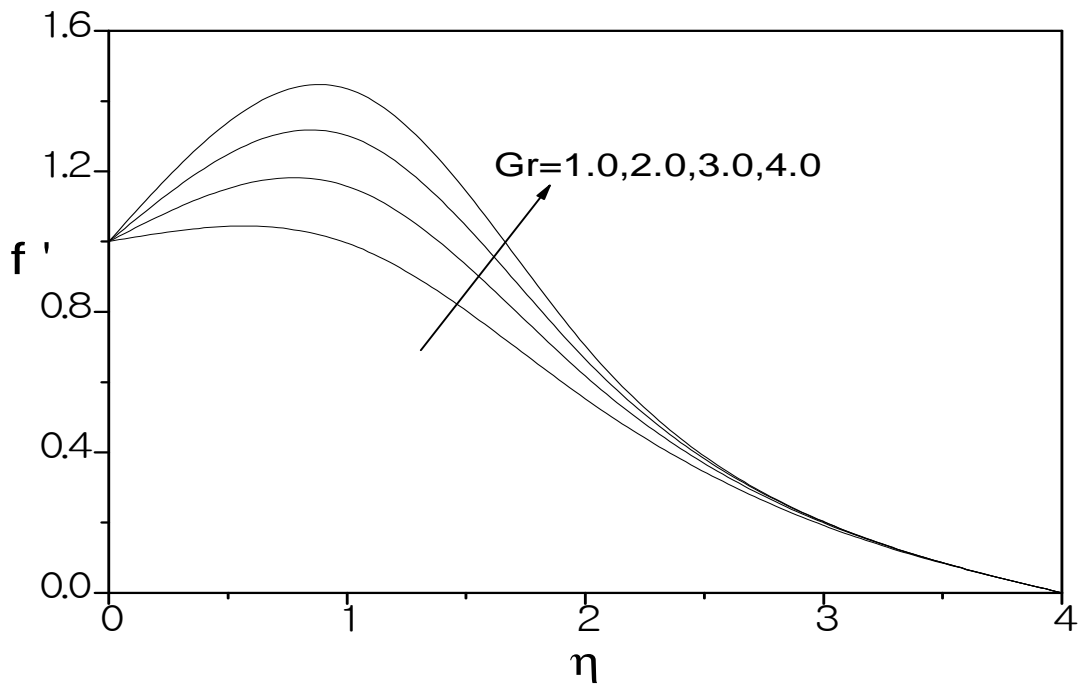


Fig.3: Variation of the velocity  $f'$  with  $Gr$  for  $Pr=0.71, Sc=0.24, Gc=1, M=0.5, S=0.2, Du=Sr=Q=0.1$ .

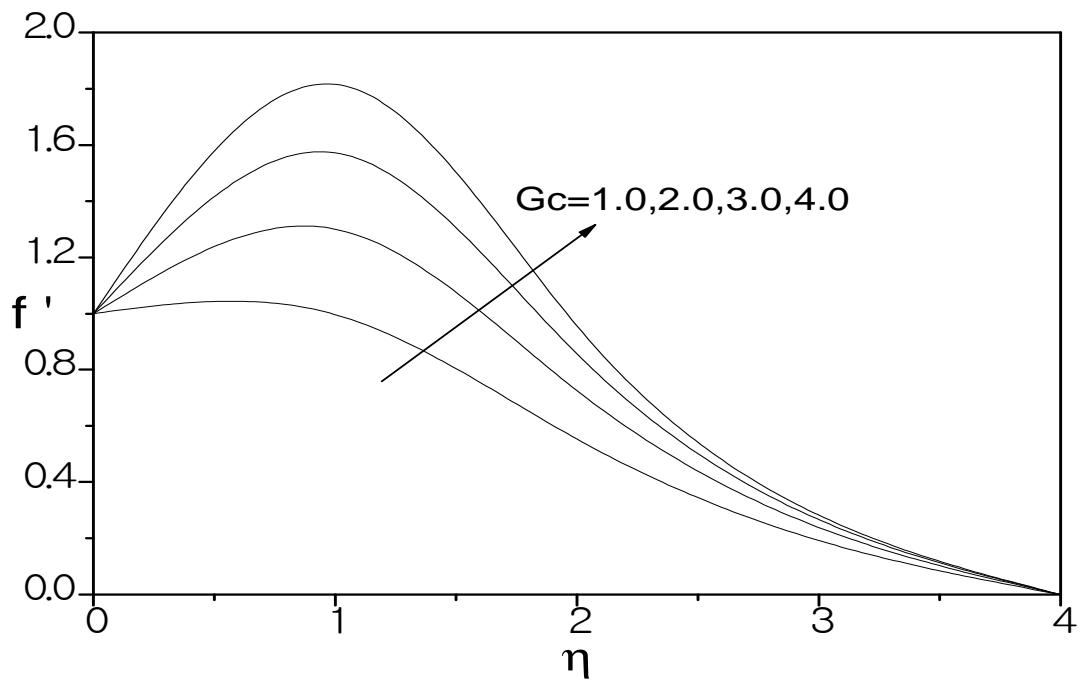


Fig.4: Variation of the velocity  $f'$  with  $Gc$  for  $Pr=0.71, Sc=0.24, Gr=1, S=0.2, M=0.5, Du=Sr=Q=0.1$ .

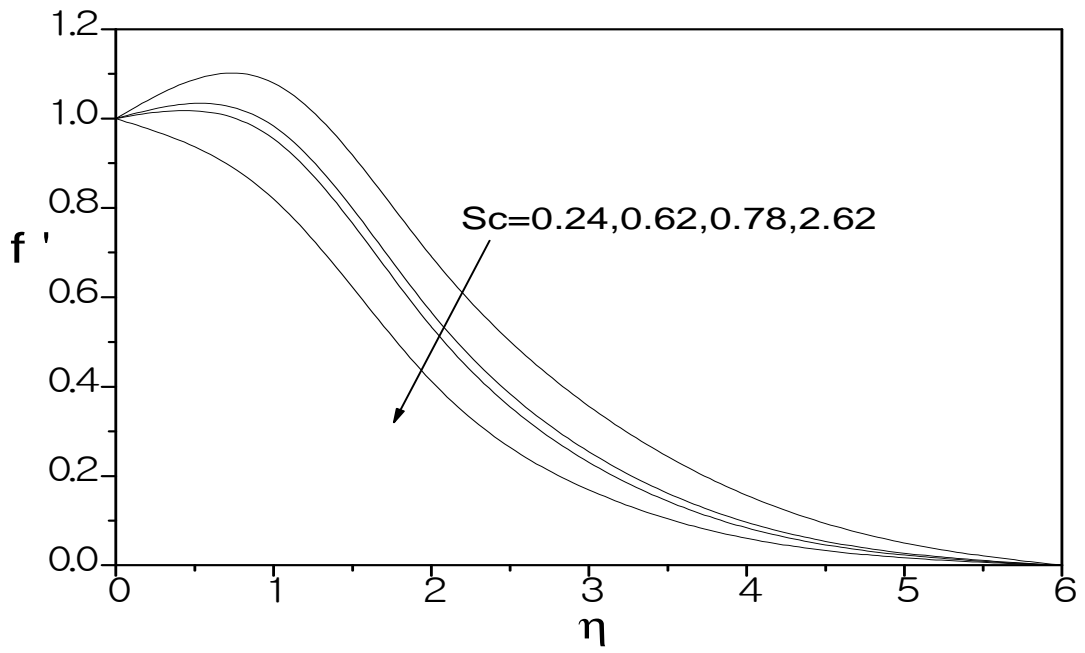


Fig.5: Variation of the velocity  $f'$  with  $Sc$  for  $Pr=0.71, Gr=Gc=1, S=0.2, M=0.5, Du= Sr=Q=0.1$ .

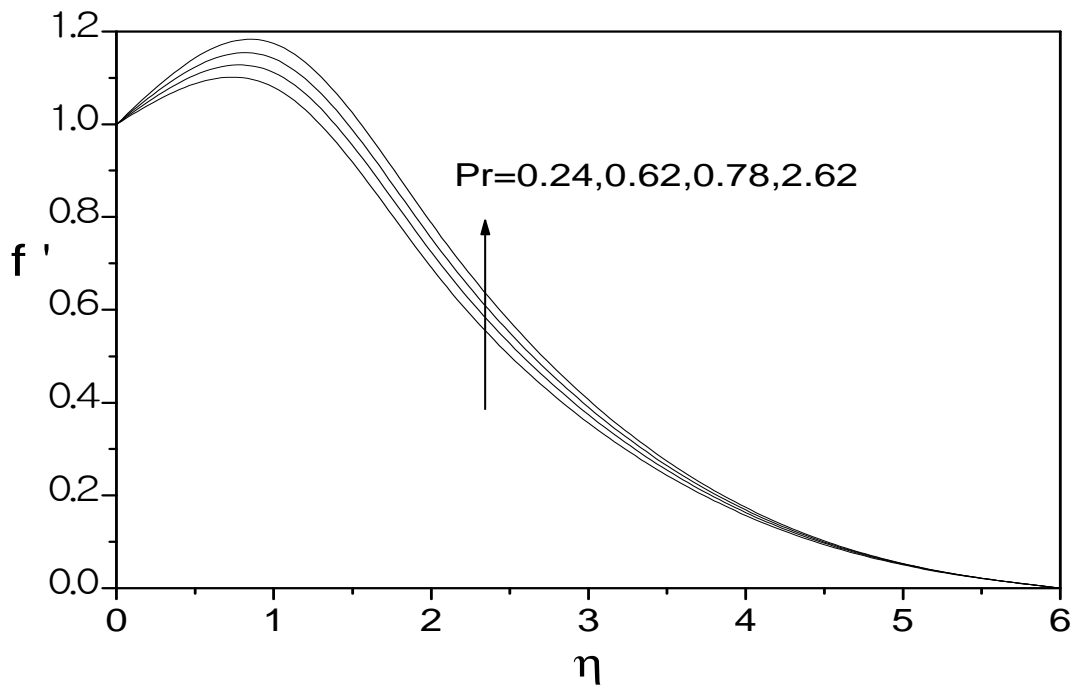


Fig.6: Variation of the velocity  $f'$  with  $Pr$  for  $Sc=0.24, Gr=Gc=1, S=0.2, M=0.5, Du= Sr=Q=0.1$ .



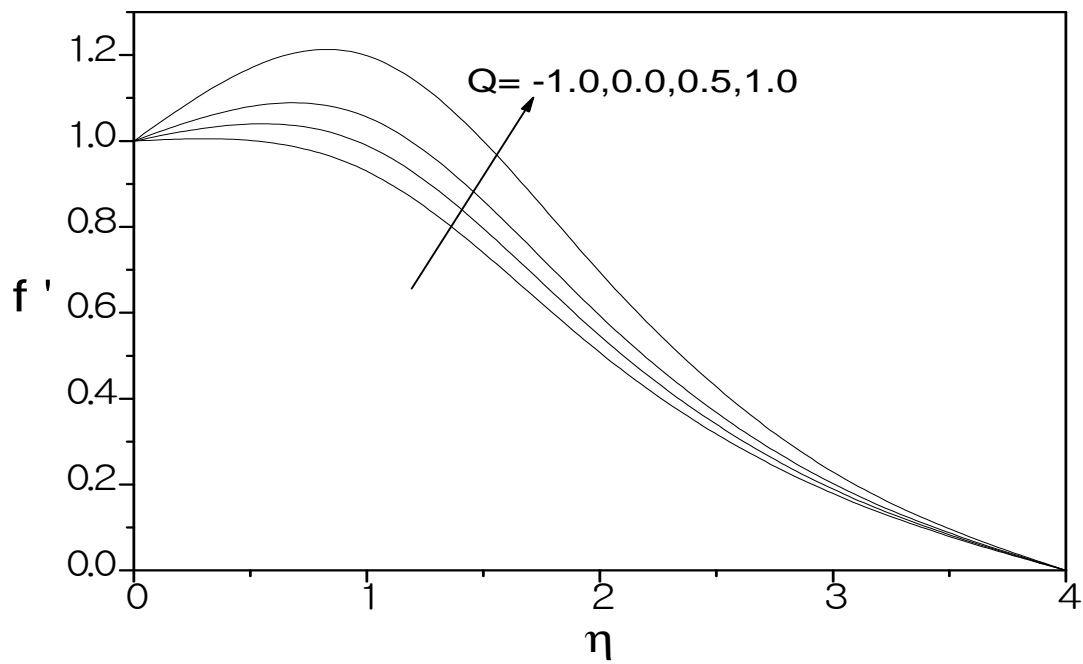


Fig.7: Variation of the velocity  $f'$  with  $Q$  for  $Sc=0.24, Pr=0.71, Gr=Gc=1, S=0.2, M=0.5, Du= Sr=0.1$

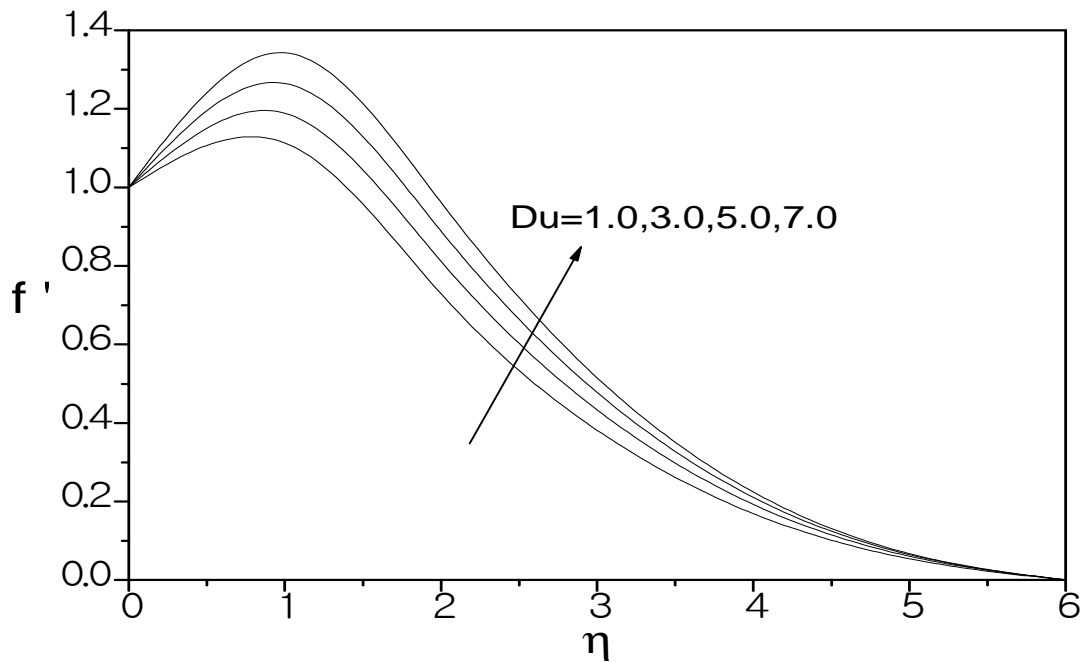


Fig.8: Variation of the velocity  $f'$  with  $Du$  for  $Pr=0.71, Sc=0.24, Gr=Gc=1, M=0.5, S=0.2, Sr=Q=0.1$ .

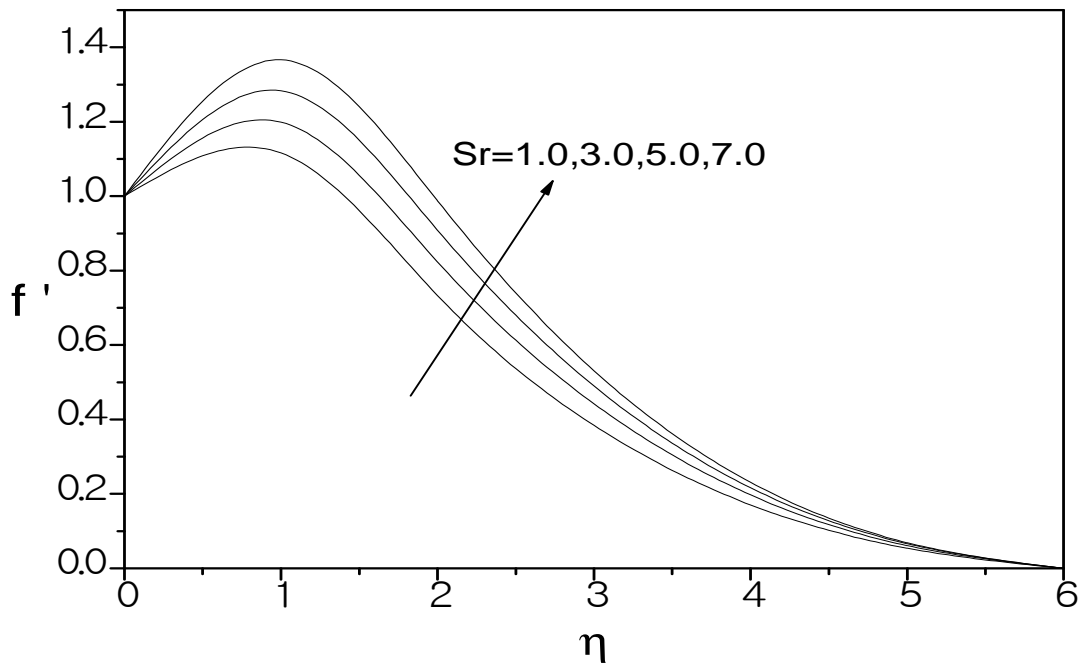


Fig.9: Variation of the velocity  $f'$  with  $Sr$  for  $Pr=0.71$ ,  $Sc=0.24$ ,  $Gr=Gc=1$ ,  $M=0.5$ ,  $S=0.2$ ,  $Du=Q=0.1$ .

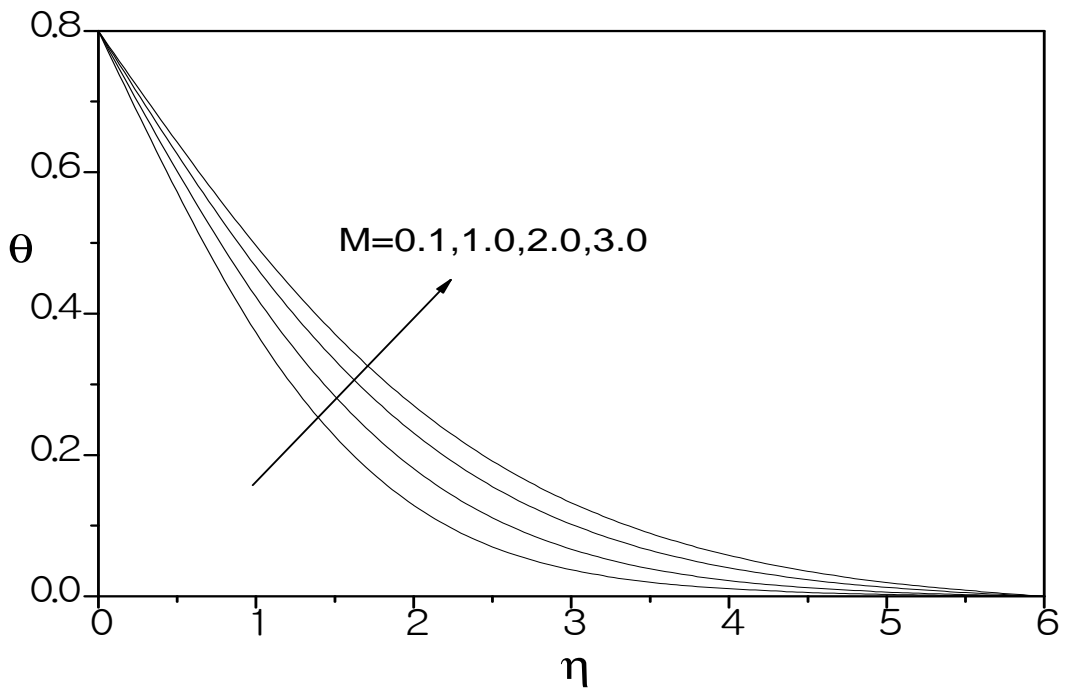


Fig.10: Variation of the temperature  $\theta$  with  $M$  for  $Pr=0.71$ ,  $Sc=0.24$ ,  $Gr=Gc=1$ ,  $S=0.2$ ,  $Du=Sr=Q=0.1$ .

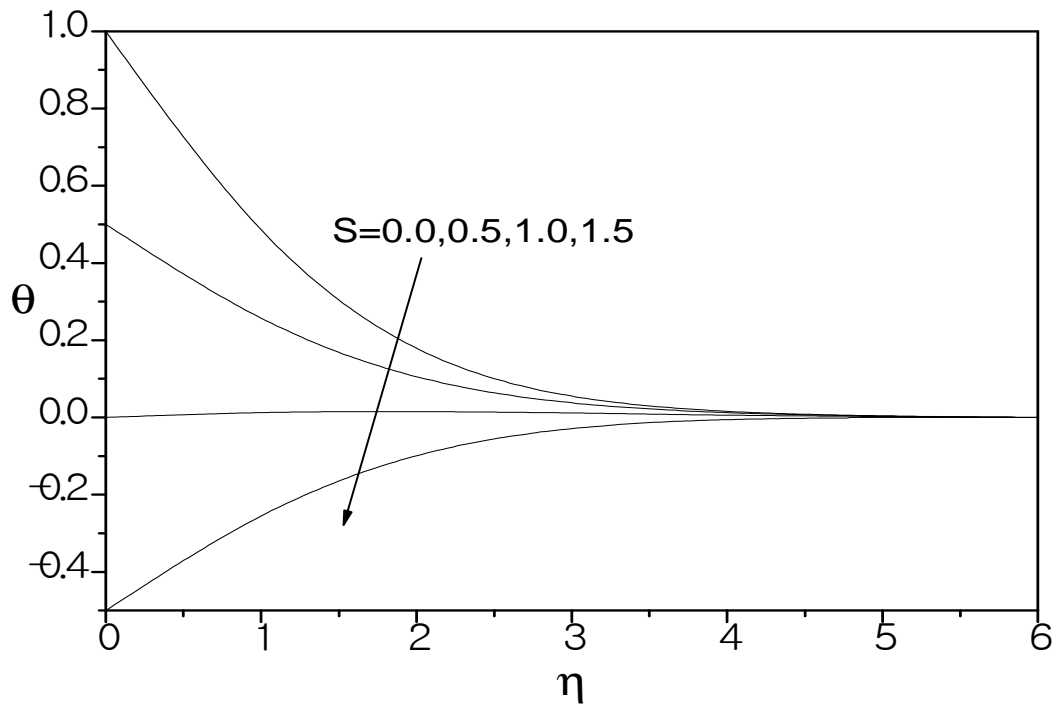


Fig.11: Variation of the temperature  $\theta$  with  $S$  for  $Pr=0.71, Sc=0.24, Gr=Gc=1, M=0.5, Du=Sr=Q=0.1$ .

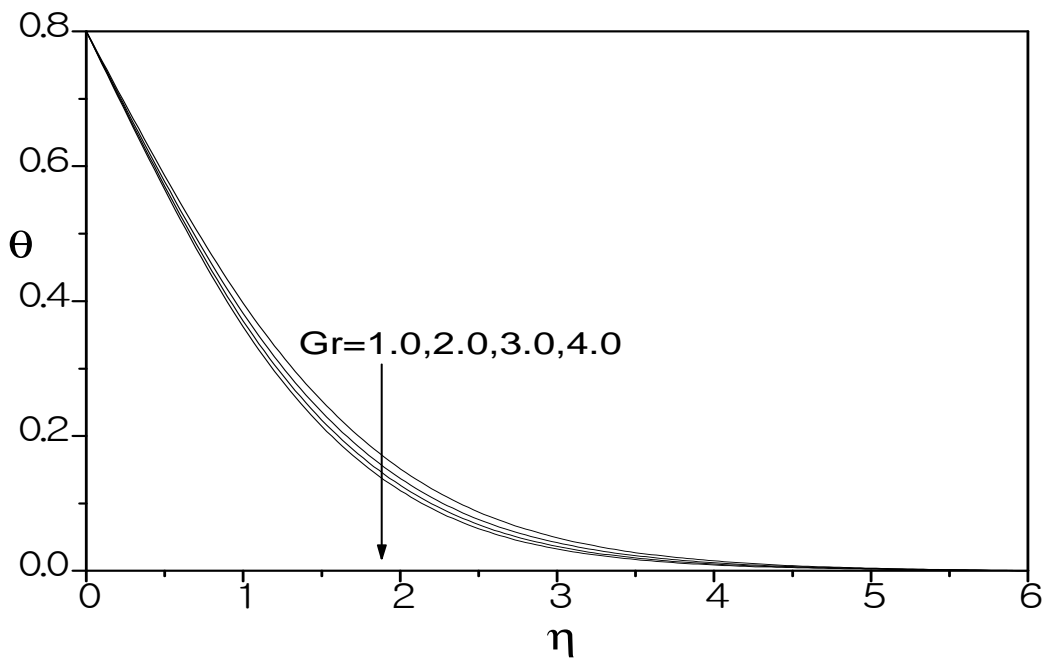


Fig.12: Variation of the temperature  $\theta$  with  $Gr$  for  $Pr=0.71, Sc=0.24, Gc=1, M=0.5, S=0.2, Du=Sr=Q=0.1$ .

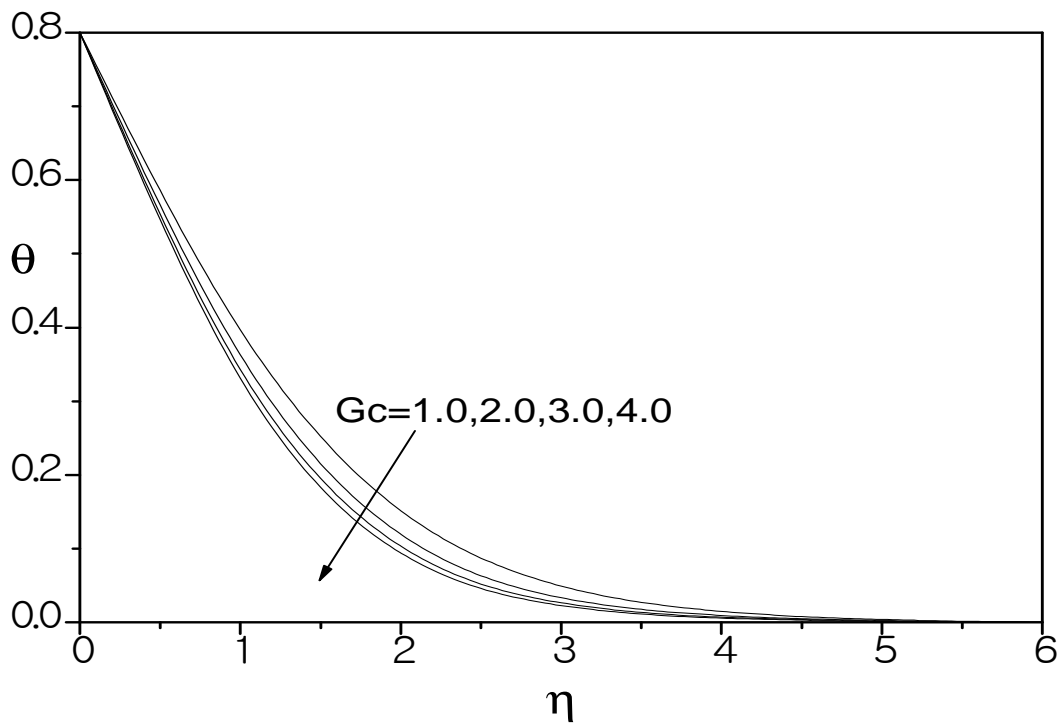


Fig.13: Variation of the temperature  $\theta$  with  $G_c$  for  $Pr=0.71, Sc=0.24, Gr=1, M=0.5, S=0.2, Du=Sr=Q=0.1$ .

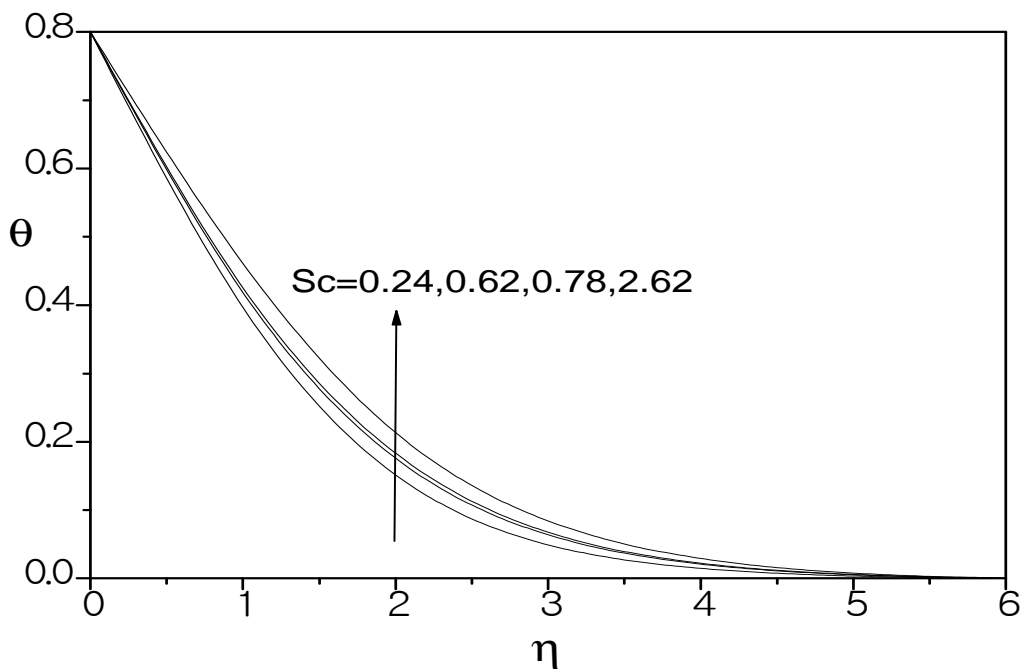


Fig.14: Variation of the temperature  $\theta$  with  $Sc$  for  $Pr=0.71, Gr=G_c=1, M=0.5, S=0.2, Du=Sr=Q=0.1$ .

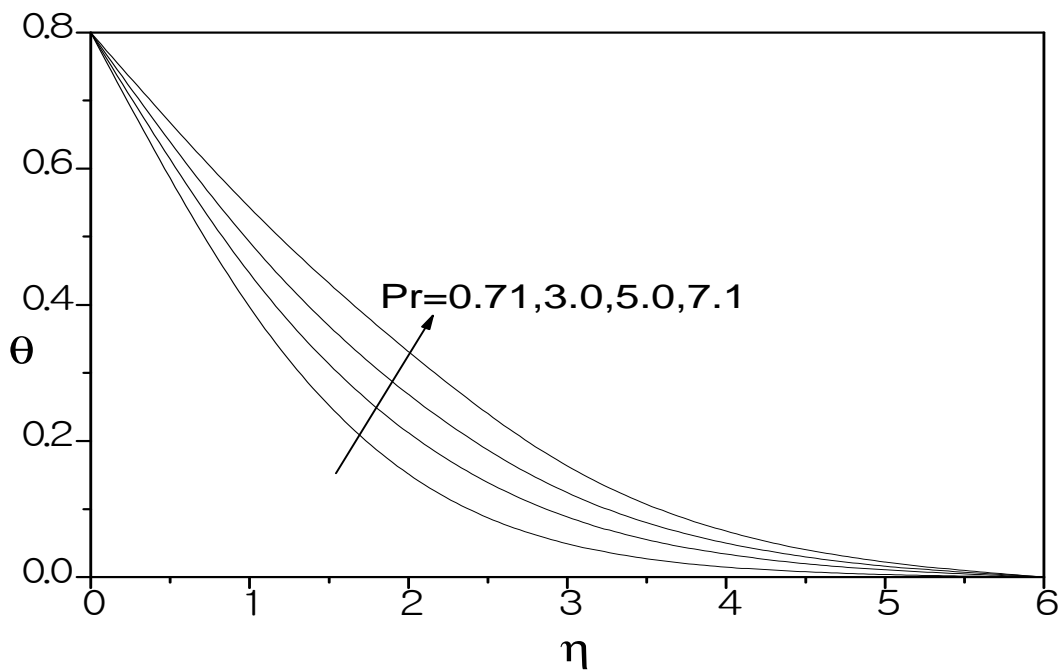


Fig.15: Variation of the temperature  $\theta$  with Pr for  $Sc=0.24, Gr=Gc=1, M=0.5, S=0.2, Du=Sr=Q=0.1$ .

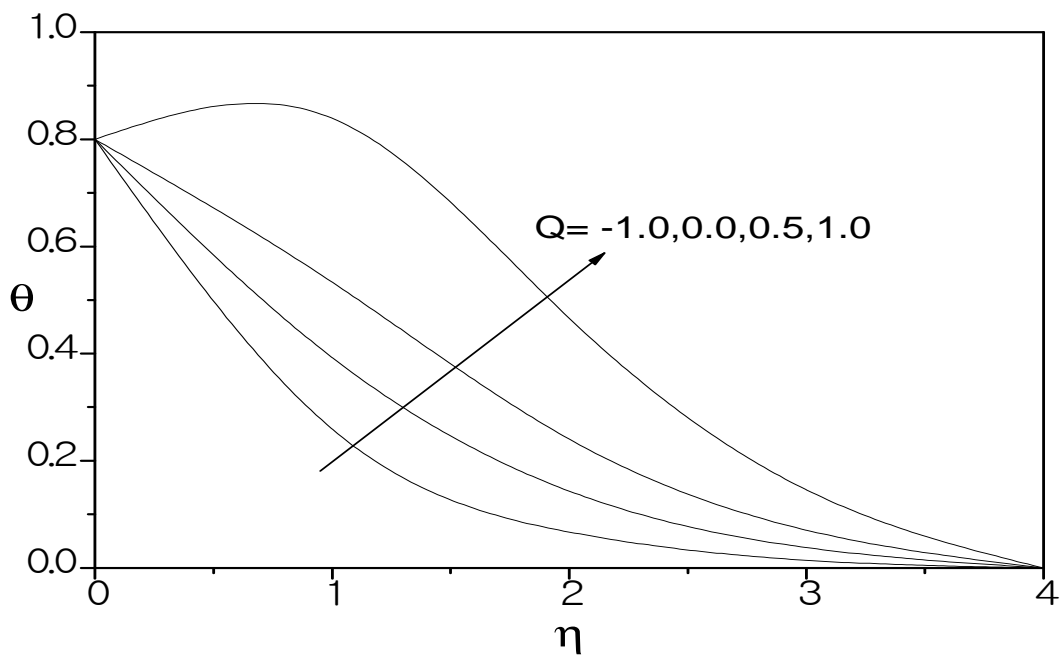


Fig.16: Variation of the temperature  $\theta$  with  $Q$  for  $Pr=0.71, Sc=0.24, Gr= Gc=1, S=0.2, Du=Sr=Q=0.1$ .

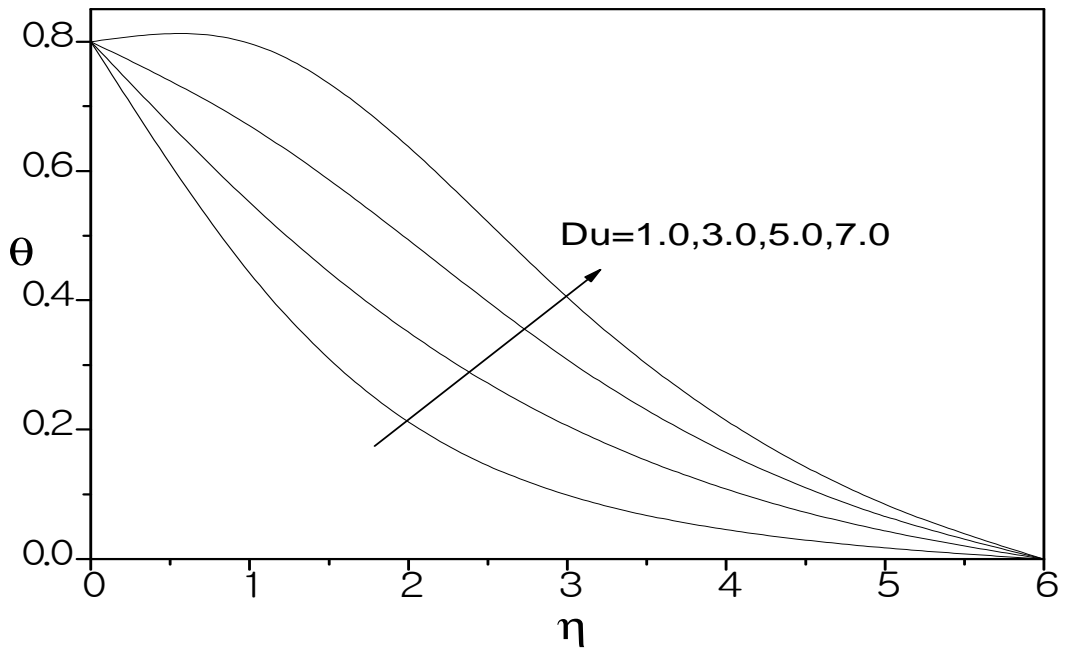


Fig.17: Variation of the temperature  $\theta$  with  $Du$  for  $Pr=0.71, Sc=0.24, Gr=1, M=0.5, S=0.2, Sr=Q=0.1$ .

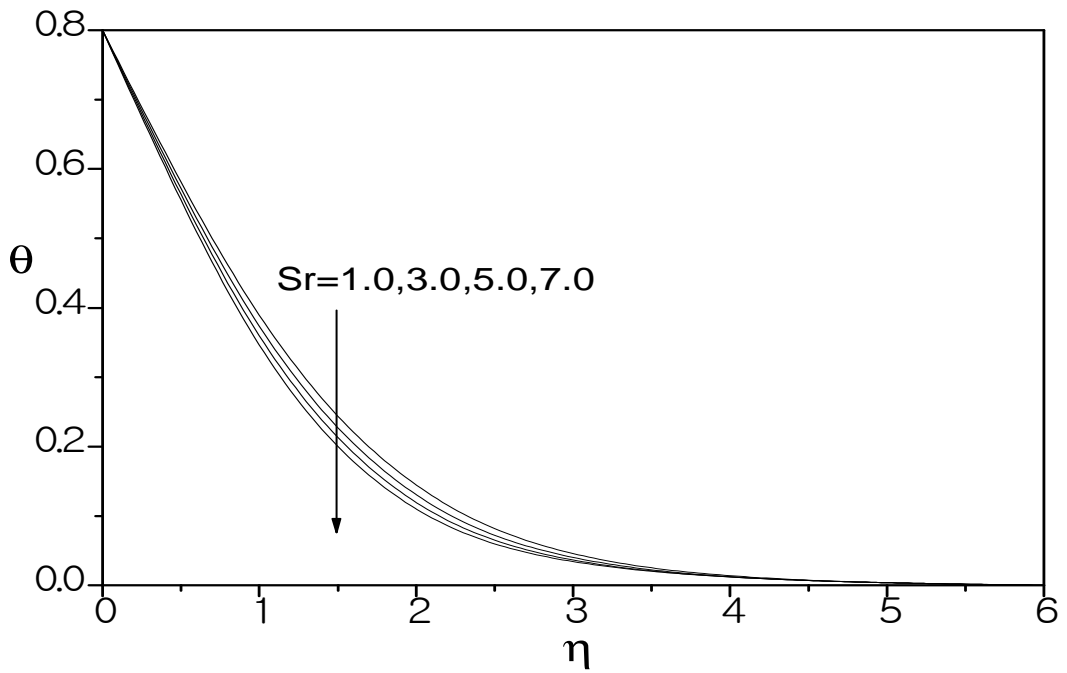


Fig.18: Variation of the temperature  $\theta$  with  $Sr$  for  $Pr=0.71, Sc=0.24, Gr=Gc=1, M=0.5, S=0.2, Du=Q=0.1$ .

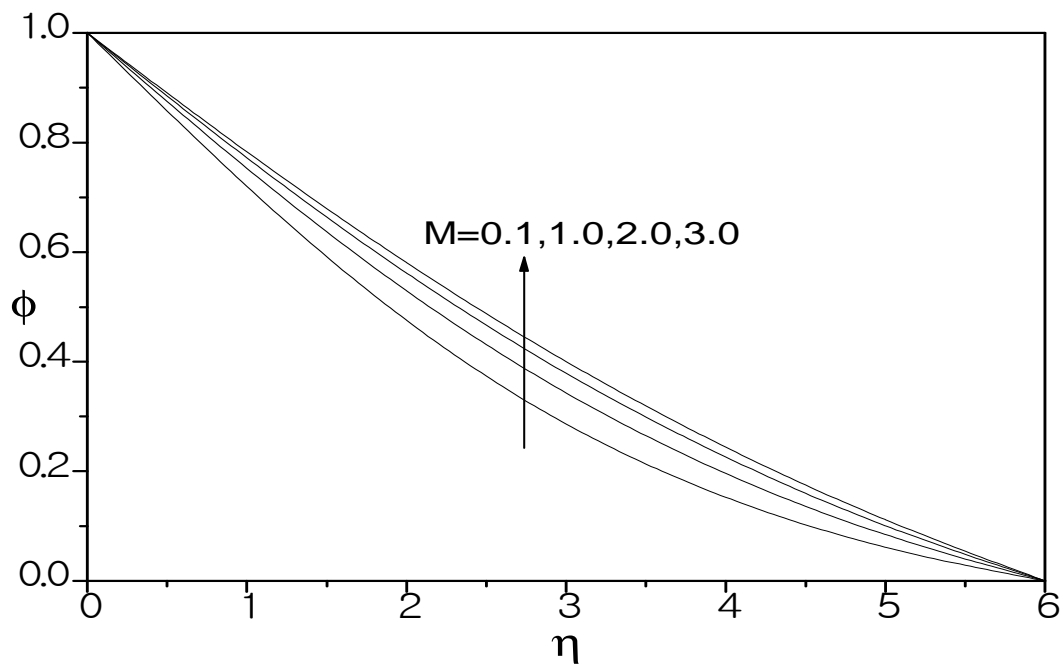


Fig.19: Variation of the temperature  $\theta$  with  $M$  for  $Pr=0.71, Sc=0.24, Gr= Gc =1, S=0.2, Du= Sr=Q=0.1$ .

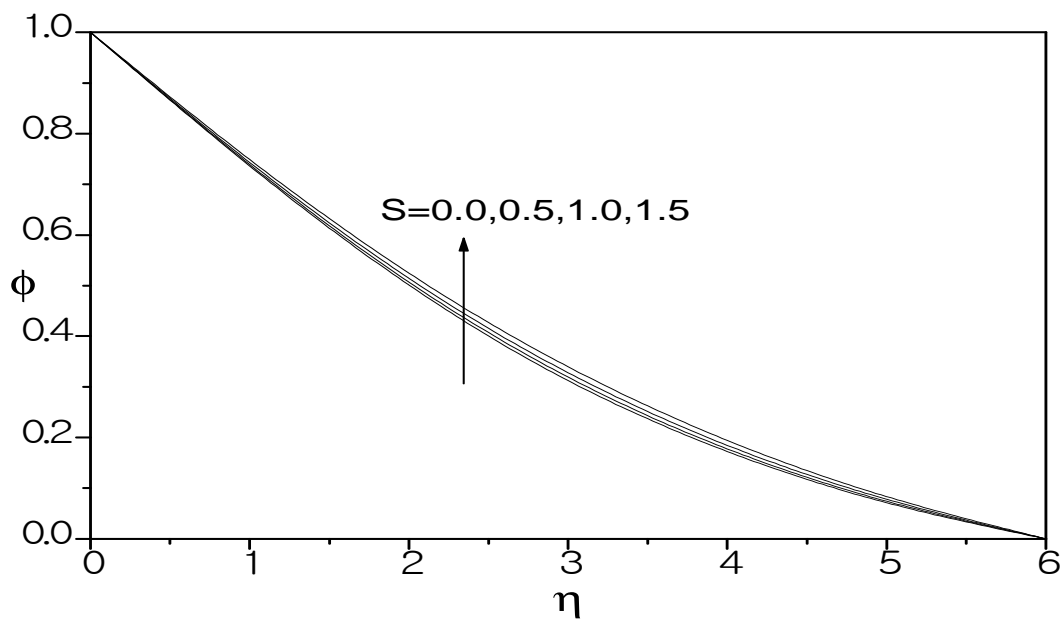


Fig.20: Variation of the temperature  $\theta$  with  $S$  for  $Pr=0.71, Sc=0.24, Gr= Gc =1, M=0.5, Du= Sr=Q=0.1$ .

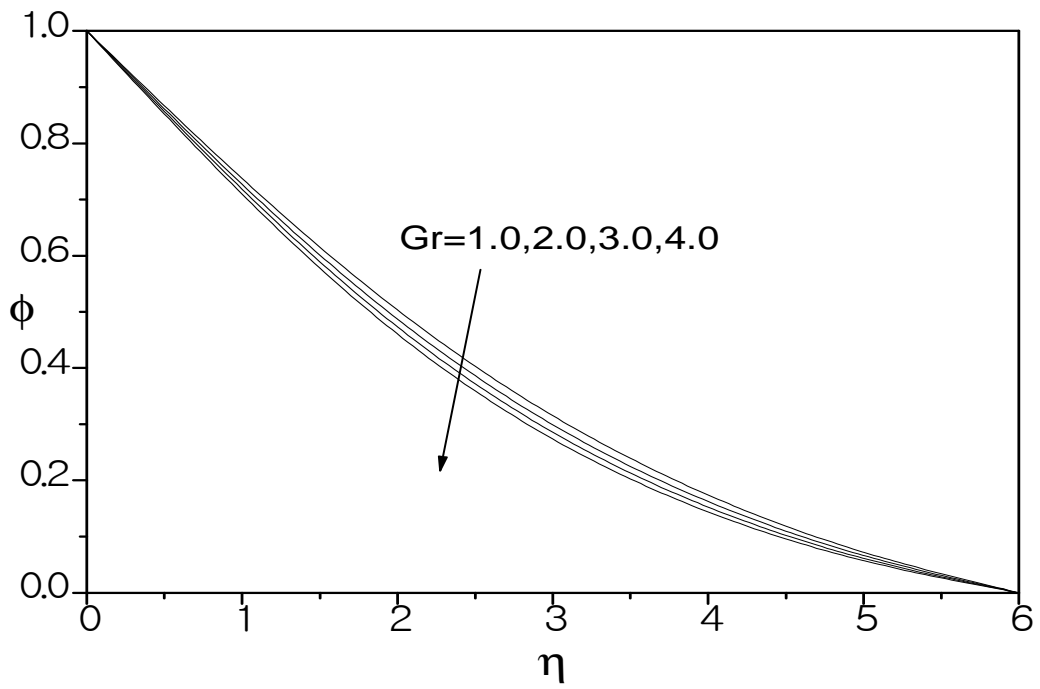


Fig.21: Variation of the concentration  $\phi$  with  $Gr$  for  $Pr=0.71$ ,  $Sc=0.24$ ,  $Gc=1$ ,  $M=0.5$ ,  $S=0.2$ ,  $Du=Sr=Q=0.1$ .

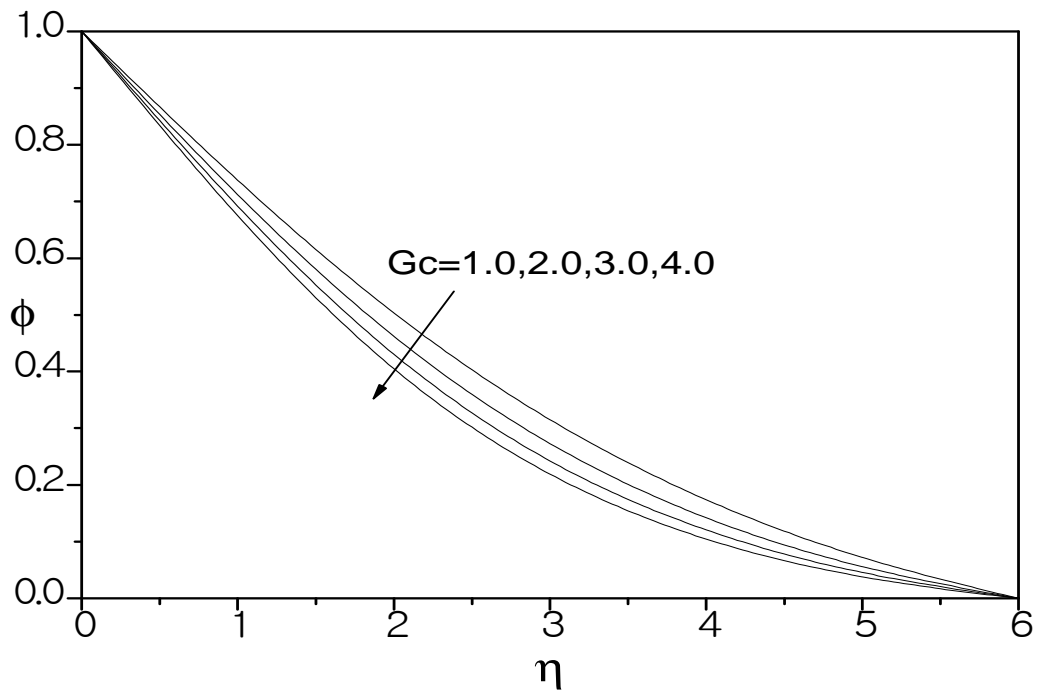


Fig.22: Variation of the concentration  $\phi$  with  $Gc$  for  $Pr=0.71$ ,  $Sc=0.24$ ,  $Gr=1$ ,  $M=0.5$ ,  $S=0.2$ ,  $Du=Sr=Q=0.1$ .



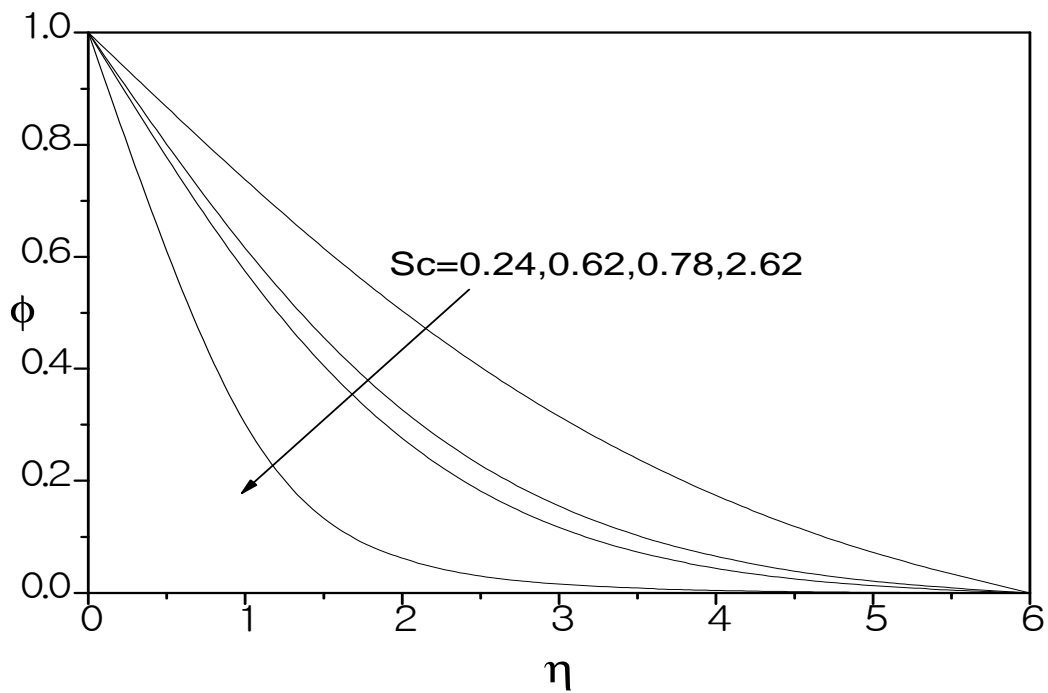


Fig.23: Variation of the concentration  $\phi$  with  $Sc$  for  $Pr=0.71, Gr=Gc=1, M=0.5, S=0.2, Du=Sr=Q=0.1$ .

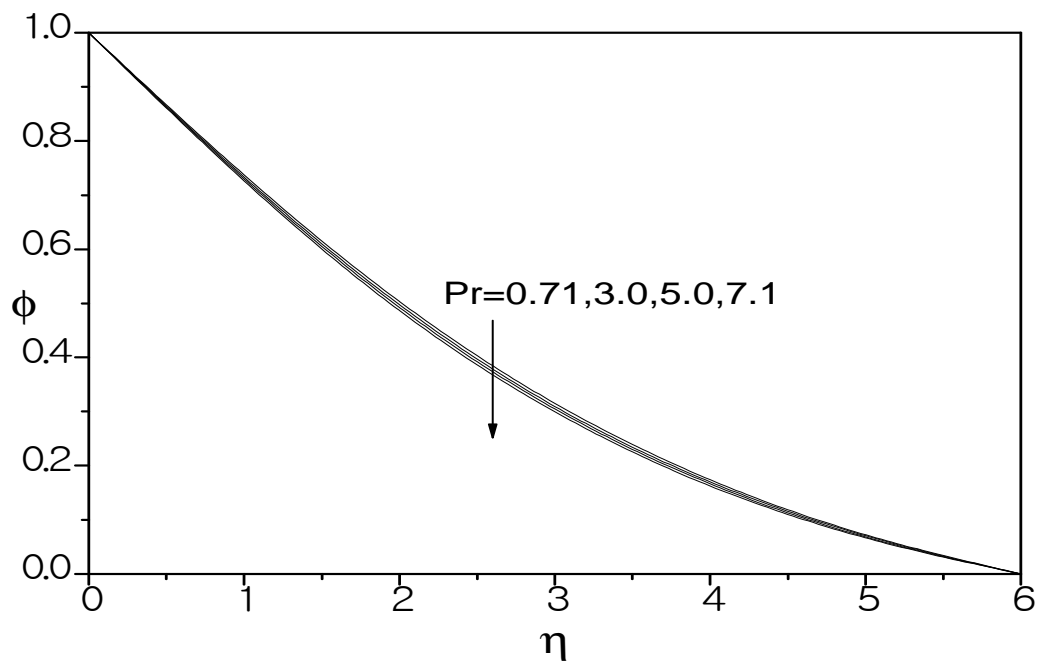


Fig.24: Variation of the concentration  $\phi$  with  $Pr$  for  $Sc=0.24, Gr=Gc=1, M=0.5, S=0.2, Du=Sr=Q=0.1$ .

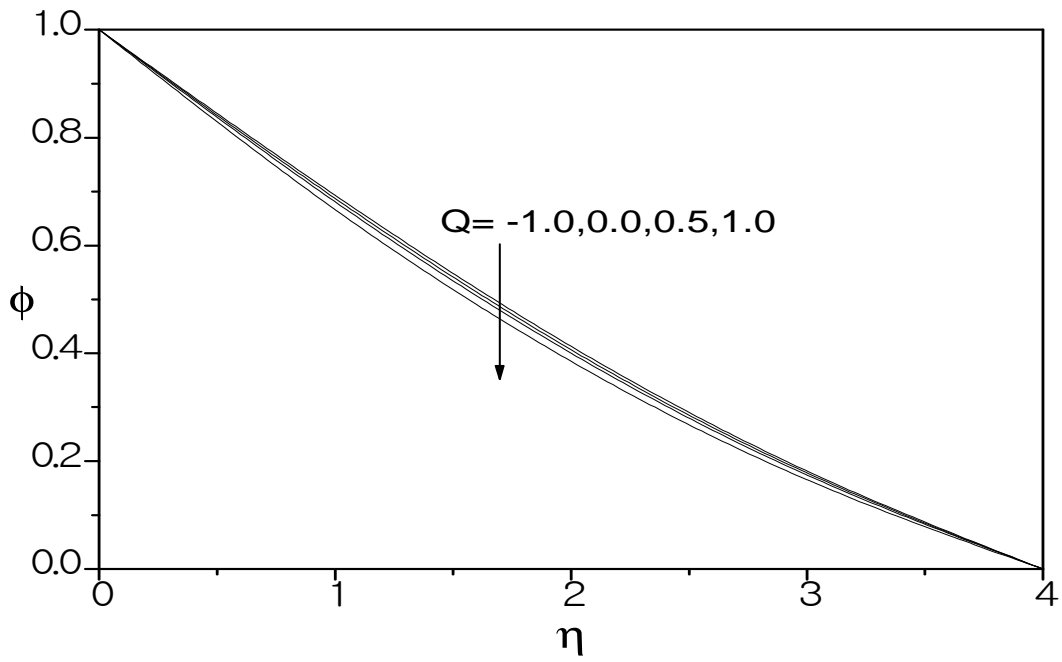


Fig.25: Variation of the concentration  $\phi$  with  $Q$  for  $Pr=0.71, Sc=0.24, Gr=Gc=1, M=0.5, S=0.2, Du=Sr=0.1$ .

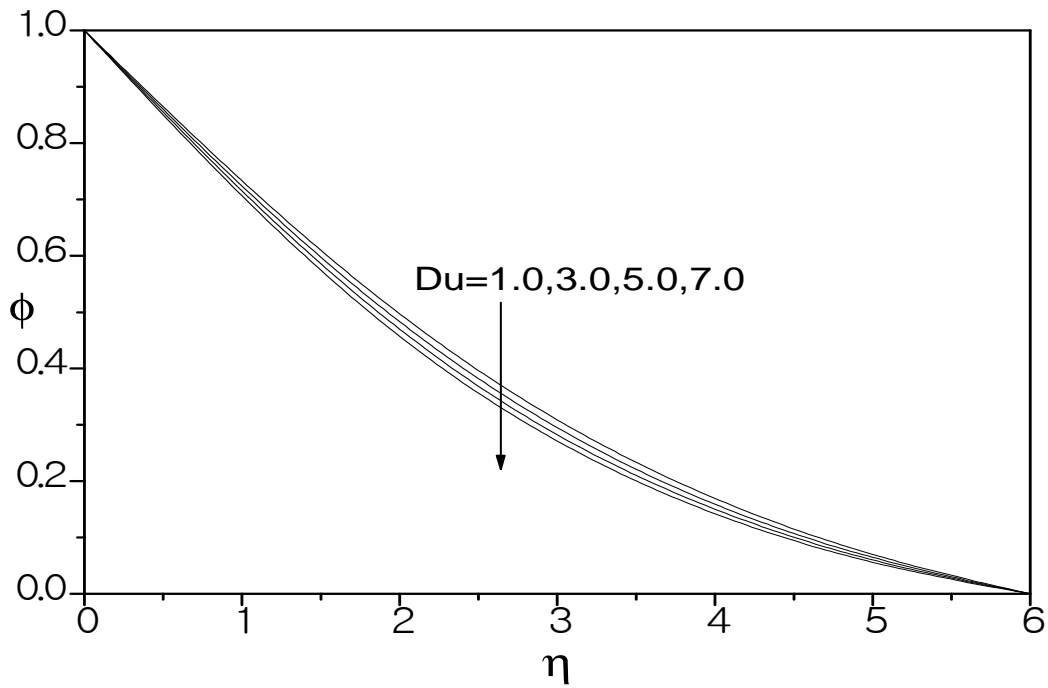


Fig.26: Variation of the concentration  $\phi$  with  $Du$  for  $Pr=0.71, Sc=0.24, Gr=Gc=1, M=0.5, S=0.2, Sr=Q=0.1$ .

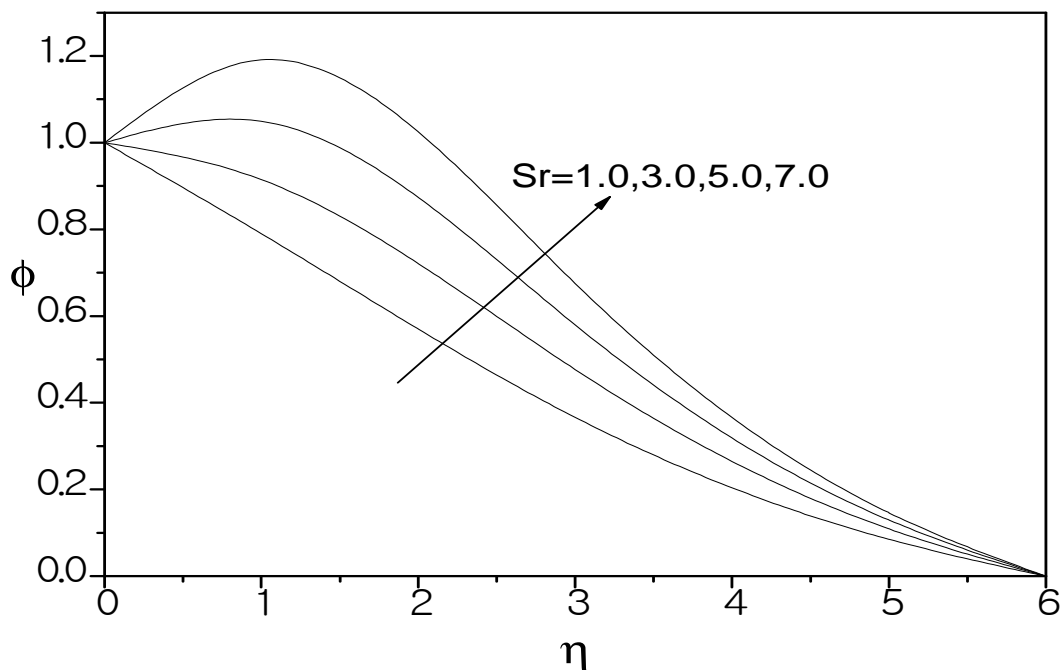


Fig.27: Variation of the concentration  $\phi$  with  $Sr$  for  $Pr=0.71, Sc=0.24, Gr=Gc = 1, M=0.5, S=0.2, Du=Q=0.1$ .

Table 1 values of  $\theta'(0)$  for different values of  $Pr$  are compared with the results obtained by Shrama and singh [15]

Pr	Shrama and singh[15]		Present Results	
	Without Q	With Q	Without Q	With Q
	$\theta'(0)$	$\theta'(0)$	$\theta'(0)$	$\theta'(0)$
0.001	-0.0264	0.9391	-0.062839	-0.0574165
0.01	-0.0805	0.8236	-0.0659358	-0.00109612
0.1	-0.2301	0.5424	-0.100842	0.0640626
1.0	-0.5671	0.0058	-0.44375	0.433445
10	-1.1662	-0.7962	-1.68029	-3.14378

Table 2 Variation of  $f''(0), -\theta'(0)$  and  $-\phi'(0)$  at the plate with  $Gr, Gc, Sc, Pr, M, Du, Sr, Q, S$ .

Gr	Gc	Sc	Pr	M	Du	Sr	Q	S	$f''(0)$	$-\theta'(0)$	$-\phi'(0)$
1.0	1.0	0.24	0.71	0.5	0.1	0.1	0.1	0.2	0.6558990	0.3179780	0.2741690
2.0	1.0	0.24	0.71	0.5	0.1	0.1	0.1	0.2	1.1643000	0.3461440	0.2869250
3.0	1.0	0.24	0.71	0.5	0.1	0.1	0.1	0.2	1.6417600	0.3687390	0.2976470
1.0	2.0	0.24	0.71	0.5	0.1	0.1	0.1	0.2	1.4096000	0.3675870	0.2987390
1.0	3.0	0.24	0.71	0.5	0.1	0.1	0.1	0.2	2.1211400	0.4045810	0.3190750
1.0	1.0	0.62	0.71	0.5	0.1	0.1	0.1	0.2	0.5432280	0.2884810	0.4196470
1.0	1.0	2.62	0.71	0.5	0.1	0.1	0.1	0.2	0.3314850	0.2273320	0.8888617
1.0	1.0	0.24	3.0	0.5	0.1	0.1	0.1	0.2	0.6105570	0.3800570	0.2696790
1.0	1.0	0.24	5.0	0.5	0.1	0.1	0.1	0.2	0.5214600	0.5426030	0.2610730
1.0	1.0	0.24	0.71	1.0	0.1	0.1	0.1	0.2	0.2079070	0.2807960	0.2581550
1.0	1.0	0.24	0.71	3.0	0.1	0.1	0.1	0.2	-0.874264	0.1897000	0.2260430
1.0	1.0	0.24	0.71	0.5	3.0	0.1	0.1	0.2	0.8386370	0.0796548	0.2930530
1.0	1.0	0.24	0.71	0.5	5.0	0.1	0.1	0.2	0.9705880	0.1080130	0.3059060
1.0	1.0	0.24	0.71	0.5	0.1	3.0	0.1	0.2	0.7681750	0.3428290	0.1420110
1.0	1.0	0.24	0.71	0.5	0.1	5.0	0.1	0.2	0.8530670	0.3599110	0.3503120
1.0	1.0	0.24	0.71	0.5	0.1	0.1	0.5	0.2	0.0959297	0.7617390	0.1999726
1.0	1.0	0.24	0.71	0.5	0.1	0.1	1.0	0.2	1.4234200	-1.2081000	0.3495820
1.0	1.0	0.24	0.71	0.5	0.1	0.1	0.1	0.4	0.5229280	0.2301570	0.2716590
1.0	1.0	0.24	0.71	0.5	0.1	0.1	0.1	0.6	0.3866810	0.1462070	0.2688060

## CONCLUSION

The present chapter analyzes the steady MHD convective flow of a viscous incompressible electrically conducting fluid along a moving, non-isothermal vertical plate by taking mass transfer, Soret and Dufour effects and heat generation or absorption into account. The governing equations are approximated to a system of non-linear ordinary differential equations by similarity transformation. Numerical calculations are carried out for various values of the dimensionless parameters of the problem. A comparison with previously published work is performed and excellent agreement between the results is found. The results are presented graphically and the conclusion is drawn that the flow field and other quantities of physical interest are significantly influenced by these parameters. The results for the prescribed skin friction, local heat and mass transfer rates at the plate are presented and discussed. It is found that the local skin-friction coefficient, local heat and mass transfer rates at the plate increase with an increase in the buoyancy forces or Soret number or Dufour number or heat generation/absorption parameter. It was observed that the local skin-friction coefficient, local heat and mass transfer rates at the plate decreases with an increase in the Magnetic parameter or Stratification parameter. As the Schmidt number increases, both the skin-friction and Nussel number decrease, whereas the Sherwood number increases. It was found that the local skin-friction coefficient and local mass transfer rate at the plate decreases but Nussel number increases with an increase in the Prandtl number.

## REFERENCES

- [1] Cheesewright, R. (1967). *Int. J. Heat Mass Trans.* Vol.10, pp.1847-1859.
- [2] Chen, C.C. Eichhorn, R. (1976). *ASME J. Heat Trans.* Vol.98, pp.446-451.
- [3] Venkatachala, B.J. Nath, G. (1981). *Int. J. Heat Mass Trans.* Vol.24, pp.1848-1859.
- [4] Uotani, M. (1987). *J. Nucl. Sci. Tech.* Vol.24, No.6, pp.442-451.
- [5] Kulkarni, A.K., Jacob, H.R., Hwang, J.J. (1987). *Int. J. of Heat and Mass Trans.* Vol.30, pp.691-698.
- [6] Ostrach, S. (1952), An analysis of laminar free convective flow and heat transfer about a flat plate parallel to direction of the generating body force. *NACA Technical Report* 1111.
- [7] Soundalgekar, V. M. (1977), *Nucelar Eng. Des.*, Vol.53, pp.309-346.
- [8] Helmy, K.A. (1998), *ZAMM*, Vol.78, pp.255-270
- [9] Zueco Jordan J. (2006), *Int. J. Eng. Sci.*, Vol.44, pp.1380-1393
- [10] Sparrow, E. M. and Cess, R. D. (1961), *Applied Scientific Research*, Vol.A10, pp.185-189.
- [11] Pop, I. and Soundalgekar, V. M. (1962), *Int.J.Heat Mass Transfer*, Vol.17, pp.85-92.
- [12] Hossain, M. A., Molla, M. M. and Yaa, L.S. (2004), *Int. J. Thermal Science*, Vol.43, pp.157-163
- [13] Chamkha, A. J. and Khaled, A. R. A. (2001), *Heat and Mass Transfer*, Vol.37, pp.117-123.
- [14] Molla, M. M., Hossain, M. A. and Yao, L. S. (2004), *International Journal of Thermal Science*, Vol. 43, pp. 157-163.
- [15] Shrama, P. R. and Gurminder Singh, (2010). *Tamkang Journal of Science and Engineering*, Vol.13, No.3, pp.235-242.
- [16] Tania, S. Khaleque and Samad, M.A. (2010). *Research Journal of Applied Sciences, Engineering and Technology*, Vol.2(4), pp.368-377, ISSN: 2040-7467.
- [17] Eckert, E.R.G. and Drake, R.M. (1972). *Analysis of Heat and Mass Transfer*. McGraw-Hill Book Co., New York.
- [18] Dursunkaya, Z. and Worek, W.M. (1992). *Int. J. Heat Mass Transfer*, Vol.35, pp.2060-2065.
- [19] Kafoussias, N.G. and Williams, E.M. (1995). *Int. J. Eng. Science*, Vol. 33, pp.1369-1376.
- [20] Maleque, Kh. A. (2010). *Tamkang Journal of Science and Engineering*, Vol. 13, No. 3, pp.235-242.
- [21] Sravan, N. Gaikwad and Shravan, S. Kamble., (2012), *Advances in applied science research*, ISSN 0976-8610, Vol. 3, pp.1426-1434.
- [22] Jeffery, A. (1966). "Magnetohydrodynamics", Oliver and Boyed, New York, USA.
- [23] Bansal, J.L. (1994). "Magnetofluidynamics of Viscous Fluids", Jaipur Publishing. House, Jaipur, India.
- [24] Schlichting, H., Gersten, K. (1999). "Boundary Layer Theory", McGraw- Hill Book Co., New York, USA.
- [25] Jain, M.K. Iyengar, S.R.K. and Jain, R.K. (1985). *Numerical Methods for Scientific and Engineering Computation*. Wiley Eastern Ltd., New Delhi, India.